ARTICLE

Infrared Absorption Intensity Analysis as a New Tool for Investigation of Salt Effect on Proteins[†]

Heng Li, Yan-yan Xu, Yu-xiang Weng*

Laboratory of Soft Matter Physics, Institute of Physics, Chinese Academy of Sciences, Beijing 100190, China

(Dated: Received on August 5, 2009; Accepted on October 28, 2009)

The native protein structures in buffer solution are maintained by the electrostatic force as well as the hydrophobic force, salt ions play an important role in maintaining the protein native structures, and their effect on the protein stability has attracted tremendous interests. Infrared spectroscopy has been generally used in molecular structure analysis due to its fingerprint resolution for different species including macromolecules as proteins. However spectral intensities have received much less attention than the vibrational frequencies. Here we report that the spectral intensities of protein amide I band, the finger prints for the protein secondary structures, are very sensitive to the local electric field known as Onsager reaction field caused by salt ions. IR absorbance thermal titrations have been conducted for a series of samples including simple water soluble amino acids, water soluble monomeric protein cytochrome c and dimeric protein DsbC and its single-site mutant G49R. We found that at lower temperature range (10−20 °C), there exists a thermal activated salting-in process, where the IR intensity increases with a rise in the temperature, corresponding to the ions binding of the hydrophobic surface of protein. This process is absent for the amino acids. When further raising the temperature, the IR intensity decreases, this is interpreted as the thermal activated breaking of the ion-protein surface binding. Applying Van't Hoff plot to the thermal titration curves, the thermodynamic parameters such as ΔH and ΔS for salting-in and ion unbinding processes can be derived for various protein secondary structural components, revealing quantitatively the extent of hydrophobic interaction as well as the strength of the ion-protein binding.

Key words: Infrared intensity, Salt effect, Fourier transform infrared spectroscopy, Secondary structure, Thermodynamic constant

I. INTRODUCTION

Infrared spectroscopy (IR) is frequently used for studies of protein structures and dynamics of the structural transitions during protein folding or function [1]. Especially, the amide I band, originating mainly from the amide C=O stretch vibrations of the peptide or protein backbone, is the chief indicator for the IR studies of the secondary structures of proteins since its conformational sensitivity has been best established [1−5]. Several advantages of time-resolved IR spectroscopic study of the amide I band, such as a higher spectral resolution compared to the circular dichroism (CD) spectroscopy for secondary structures [6,7], and a better temporal resolution than the stopped-flow technique, have made IR spectroscopy a technique of choice, for example, for numerous dynamic studies of protein folding [8−10]. On the other hand, one of the disadvantages for investigations of protein structural properties with IR spectroscopy is that the most used salts in buffer strongly affect the frequency and intensity of amide I band, interferring the assignment of the IR finger prints for the secondary structural components. To avoid the complexity induced by the salt effect, most of the researchers chose to conduct the IR spectroscopic study of IR in D_2O [11,12], apparently the condition in D_2O is different from that in buffer, and the conclusions obtained thereby may not be extended to those *in vivo*. Consequently, it is necessary to clarify the salt effect on protein structures by understanding the salt-induced frequency and absorbance changes in amide I band.

Recent experimental studies and theoretical simulations [13−15] show that the addition of salt introduces three effects which can affect the conformation of proteins further causing the corresponding changes in amide I band: (i) non-specific screening of the electrostatic interactions in proteins, (ii) specific ion binding to proteins, and (iii) ions affecting the water structure,

[†]Part of the special issue for "the Chinese Chemical Society's 11th National Chemical Dynamics Symposium".

*Author to whom correspondence should be addressed. E-mail: yxweng@aphy.iphy.ac.cn

which results in an increase or decrease in the hydrophobic interactions of proteins [16,17]. For understanding this complexity Reiner *et al.* studied the influence of salts on the conformational equilibrium between the active and the inactive photoproduct states of rhodopsin, *i.e.*, Meta II and Meta I [13,18]. Kazumasa *et al.* also investigated the salt-dependent monomer-dimer equilibrium by amide I spectra [19]. All the investigations were based on the salt effects on the amide I frequency shifts of proteins. However, spectral intensities have received much less attention than the vibrational frequencies for the difficult in determination of spectral intensity change, even though the intensities are much important in determining the appearance of the experimental amide I spectral contours and the thermodynamic details of the interaction between proteins and salt ions.

In this work, we proposed the amide I absorption intensity change of proteins solution in the presence of salt as a quantitative parameter to illustrate the ion effect on the protein stability. To the best of authors' knowledge, this is the first investigation of salt effect on the stability of protein secondary structures by means of IR intensity. We conducted the temperature dependent IR spectroscopic study of a series of samples including simple water-soluble amino acids, water-soluble protein cytochrome c and dimeric protein DsbC and its single-site mutant monomeric G49R. The corresponding amide I absorbance thermal titrations in both D_2O and buffer were acquired. Results show that (i) IR absorbance of proteins in the salt solution is more intense than in D_2O, this is interpreted as the local electric field effect on the transition dipole moment of the amide I; (ii) there are two successive temperature-dependent processes for amide I intensity change in the salt solution, the first is an increase of amide I absorption intensity against the raising of the temperature in the lower temperature range (10−20 °C), corresponding to the ions binding of the hydrophobic protein surface. This process is absent for the amino acids. The second is a decrease of amide I absorption intensity when further raising the temperature, this is interpreted as the thermal activated breaking of the ion-protein surface binding. In addition, applying Van't Hoff plot to the thermal titration curves, we have derived the thermodynamic constants of various protein secondary structural components for salting-in and ion unbinding processes, which quantitatively reveal the extent of hydrophobic interaction as well as the strength of the ion-protein binding.

II. MATERIALS AND METHODS

A. Chemicals

L-glutamic acid (Glu, purity ∼99.0%) and horse heart cyt c (c-7752, purity ∼99.0%) were purchased from Sangon Co. and Sigma (St. Louis, MO), respectively. Recombinant DsbC (dimer) and G49R (single-point mutant monomer of DsbC) were made according to reports by Ke *et al.* [20]. All samples were dissolved in 99.9% D_2O or in phosphate buffer (containing 50 mmol/L K_2DPO_4/KD_2PO_4, pD≈7) at concentration of ∼12.5 g/L which all were kept in an airtight bottle for 24 h. The value 0.4 was added to the pH reading to give pD values for the D_2O solutions [21]. pD value of Glu, cyt c, DsbC, and DsbC-G49R in D_2O solution are 5.2, 7.0, 6.2, and 6.2 respectively. The α-COOH of Glu solution is almost completely dissociated because pK_{a2} value of Glu is 4.25 [21]. The structures of DsbC family proteins are hardly affected by normal reaction pH (6.0−8.0) [22].

B. FTIR spectroscopy

Temperature-dependent FTIR (Fourier transform infrared spectroscopy) spectra were collected on a spectrometer (ABB-BOMEM, Bureau, Québec) equipped with a Globar source, a KBr beam splitter, and a liquid nitrogen cooled broad band mercury-cadmium-telluride (MCT) detector. A two-compartment CaF_2 sample cell with a 56-μm-thick Teflon spacer was used for protein and reference solution, respectively. The measurements were performed in a home-made vacuum chamber with a controlled temperature at accuracy of ±0.1 °C by water circulation. Each spectrum at different temperature with equilibrium time of 20 min is an average of 40 scans. Reference spectral subtraction was carried out to give a straight baseline in the spectral region of 1750−2000 cm^{-1}. A linear baseline was subtracted from each spectrum [6,23].

III. RESULTS AND DISCUSSION

Figure 1 represents FTIR spectra of Glu, cyt c, DsbC, and G49R in D_2O and salt solution at 20 °C. The peaks determined by the second derivative spectra hardly shift in both solutions (less than 3 cm^{-1}), while the FTIR spectrum of each sample in salt solution almost has the same profile as that in D_2O except for its absorption intensity. The facts reveal that there is almost no secondary structure change between two solutions. It is obvious that IR absorption intensities of Glu, cyt c, DsbC, and G49R in salt solution are larger than those in D_2O at the indicated temperature. It has been reported that solvent dielectric effect would screen the electrostatic interactions between groups of the protein, known as nonspecific screening effect [24,25]. When proteins dissolve in salt solution, the salt ions form screening around protein, which supplies a stable external electric field to polarize the dipole of the C=O groups, and the C=O dipole moment induces a dipole moment of opposite direction in the surrounding medium. Polarization of the medium in turn polarizes the charge distribution of the

DOI:10.1088/1674-0068/22/06/556-562

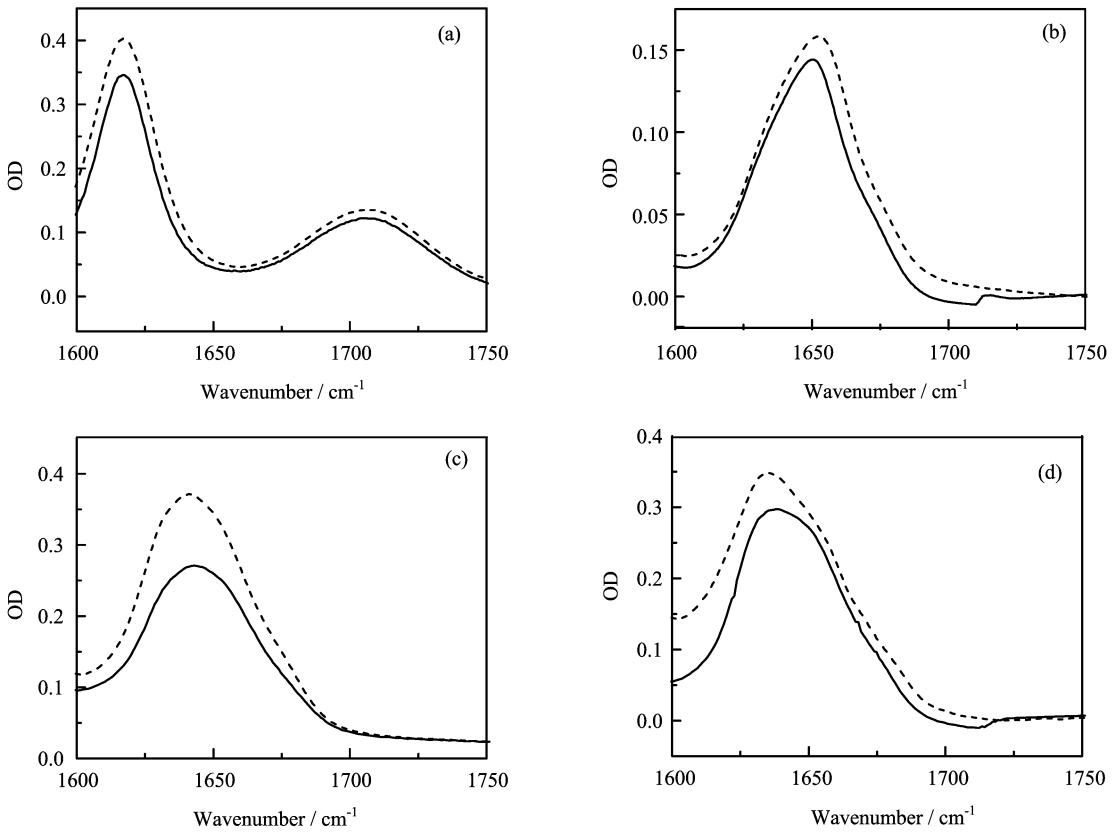

FIG. 1 FTIR absorption spectra of Glu (a), cyt c (b), G49R (c), and DsbC (d) dissolved in D_2O and phosphate buffer with concentration of 12.5 g/L at 20 °C. The amide I band intensities of the sample dissolved in buffer (dashed line) are always larger than that in D_2O (solid line).

C=O group in the solvent. Treating this mutual polarization in a self consistent manner leads to the Onsager reaction field model (see Fig.2). The reaction field $\vec{R}$ generated in this manner is proportional to the molecular dipole moment μ and inversely proportional to the third power of the radius a_0 of the solute cavity in the equation (ε: dielectric constant of medium) as follows [26−28]:

$$\vec{R} = \frac{2(\varepsilon - 1)}{2\varepsilon + 1} \frac{\vec{\mu}}{{a_0}^3} \tag{1}$$

According to Buckingham infrared intensity theory, the observed IR absorption intensity $A_{\text{solv.}}$ can be expressed as [29−31]:

$$A_{\text{solv.}} = \frac{9n^3}{(2n^2+1)^2} \frac{8\pi^3 NB}{3h} \overline{\mu'^2} \tag{2}$$

Where n is the refractive index of medium, N is the number of molecules in unit volume, B is the Boltzmann constant, h is the Planck constant, and $\overline{\mu'^2}$ is the mean value of the square of the dipole moment derivative of the solute molecule and its near neighbors in a sphere surrounding it. Therefore, increased IR absorption intensities can be observed in Fig.1, when salt ions

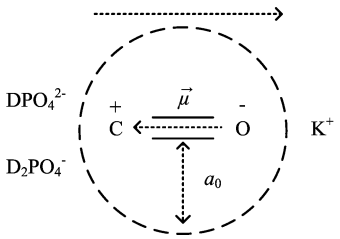

FIG. 2 Schmatic diagram of Onsager reaction field model.

lead to the larger reaction field, at the same time, the transition dipole moment of C=O group become larger.

Figure 3 (a) and (c) show the thermal titration curves at the indicated wavenumbers for Glu and G49R in D_2O and salt solution respectively. Because the thermal titration curves of cyt c, G49R, and DsbC are similar, here we just show the data of G49R as an example. Figure 3(c) reveals that the thermal titration curve of G49R exhibits an intensity increase process (10−20 °C) in salt solution compared with that in D_2O, while this process is obviously absent in that for Glu. The most obvious structural difference between G49R and Glu is

DOI:10.1088/1674-0068/22/06/556-562

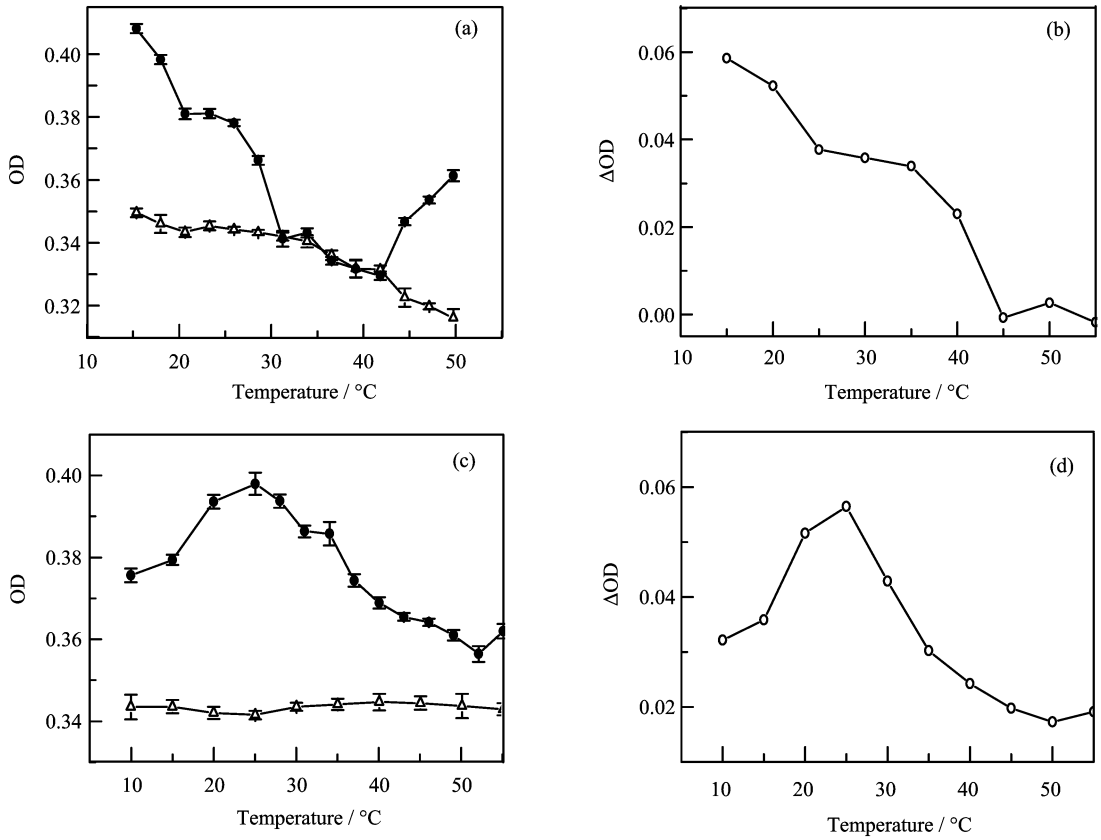

FIG. 3 Thermal titration curves of Glu (a) and G49R (c) in D_2O (△) and buffer (•) and salt effect curves (○) on Glu (b) and (d) are the difference thermal titration curves between samples in salt solution and in D_2O (salt effect curves). The error bars are expressed as ±S.D. (n=3).

that the former contains secondary structures, which makes some carbonyls group buried in hydrophobic domains of proteins while the latter is fully exposed to the solvent molecules. In the salt solution, ion effect on hydrophobic surface of proteins must be considered, which mainly includes salting-in effect in this temperature range [32,33]. If water-ion interaction is weaker than water-water interaction, salt ions are more apt to bind with hydrophobic surface of protein and while water molecules mainly interact with hydrophilic domains, which would increase the solubility of protein and stabilize proteins, in general, this is termed as salting-in process [32]. In the salting-in process, both the temperature and the charge density of ions could change the strength of water-ion interaction. The higher temperature, or, the smaller charge density, the weaker the water-ion interaction [32], which leads to a preferential binding of ions to the protein surface, giving rise to an increased IR absorbance.

Under the experimental condition, the same salt is used for all the solution samples and the charge density change can be neglected in the experimental temperature range. When raising temperature gradually as indicated in Fig.3(c), thermal effect would weaken water-ion interaction to some extent, which leads to salt ions being preferentially bound to hydrophobic surface of proteins, and surround the protein surface area as much as possible, forming stronger screening to electrostatic interaction between groups in proteins. In turn, the ionic screening could supply external electric field to polarize the electronic distribution of C=O bond, and therefore increases the reaction field of C=O bond [34]. Therefore the IR absorption intensity change resulting from salt effect increases with temperature rising, as shown in the rising phase of Fig.3(d). However when temperature exceeds the maximum IR absorbance as at 20 °C for G49R, thermally activated motion of salt ions becomes significant, which reduces the ion-protein surface bound and hence the ionic screening of protein surface, that is, the unbinding between ion and protein happens, which leads to the decrease of amide I absorption intensity as shown in the deceasing phase of Fig.3 (b) and (d). Obviously, external electric field generated by the ion binding on the protein becomes weaker gradually as further raising the temperature.

Both salting-in and unbinding processes can be described by a two-state equilibrium as follows:

Salting-in process:

DOI:10.1088/1674-0068/22/06/556-562

$$\begin{aligned}&[\text{Native state}] \xrightarrow{k_{+1}^{\text{in}}} [\text{Salting-in state}]\\ &[\text{Salting-in state}] \xrightarrow{k_{-1}^{\text{in}}} [\text{Native state}]\end{aligned} \tag{3}$$

Unbinding process:

$$\begin{aligned}&[\text{Binding state}] \xrightarrow{k_{+1}^{\text{in}}} [\text{Unbinding state}]\\ &[\text{Unbinding state}] \xrightarrow{k_{-1}^{\text{in}}} [\text{Binding state}]\end{aligned} \tag{4}$$

where native state represents the low-temperature state at which the salt ions can hardly act on the hydrophobic surface of proteins, both salting-in and binding states imply that strong electrostatic interaction exists between salt ions and proteins, and unbinding state indicates that electrostatic interaction between salt ions and proteins becomes weaker.

For salting-in process, equilibrium constant K^{in} is written as:

$$K^{\text{in}} = \frac{k_{+1}^{\text{in}}}{k_{-1}^{\text{in}}} = \frac{[\text{Salting-in state}]}{[\text{Native state}]} \tag{5}$$

where the concentration ratio of salting-in state over that of the native state of proteins at a given temperature can be derived by normalized IR absorption intensities according to Beer-Lambert law, $I_{\text{nor}}^{\text{in}}$ is normalized IR absorption intensity

$$\frac{[\text{Salting-in state}]}{[\text{Native state}]} = \frac{I_{\text{nor}}^{\text{in}}}{1 - I_{\text{nor}}^{\text{in}}} \tag{6}$$

Incorporating the above ratio into the thermodynamic relation $-R\ln K^{\text{in}}=\Delta H^{\text{in}}/T-\Delta S^{\text{in}}$, where ΔH^{in} and ΔS^{in} denote the molar enthalpy and molar entropy changes, and R is gas constant, we have:

$$\ln\frac{I_{\text{nor}}^{\text{in}}}{1 - I_{\text{nor}}^{\text{in}}} = -\frac{\Delta H^{\text{in}}}{R}\frac{1}{T} + \frac{\Delta S^{\text{in}}}{R} \tag{7}$$

Figure 4(a) plots the $\ln[I_{\text{nor}}^{\text{in}}/(1-I_{\text{nor}}^{\text{in}})]$ quantity against $1/T$ (Van't Hoff plot) [35]. By linear fitting, the thermodynamic constants ΔH^{in} and ΔS^{in} for Eq.(3) were derived. And the fitting results of ΔH^{in} and ΔS^{in} for three kinds of secondary structures derived at different wavenumbers are listed in Table I for G49R. All ΔH^{in} values are positive within experimental error, which indicates that salting-in of G49R at lower temperature is an endothermic process, and the increased enthalpy is mainly due to the breaking of the hydrophobic interaction. Therefore we tentatively proposed that ΔH^{in} as a quantitative indicator for the hydrophobic interaction of the protein structural segments. As shown in Table I, the ΔH^{in} value of α-helix in the salting-in process is larger than that of the other two structures, which means that salt ions into α-helix structure need more energy, corresponding to a stronger hydrophobic interaction for α-helix structure. For cyt c and DsbC,

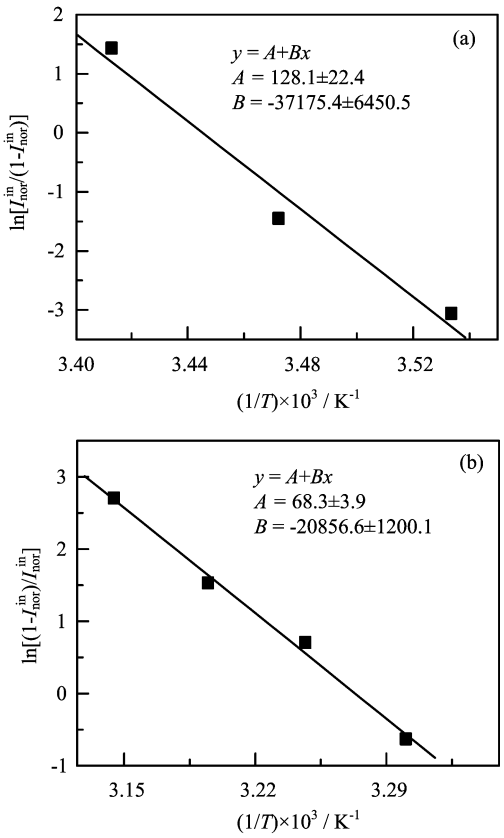

FIG. 4 Van't Hoff plots of G49R in the process of salting-in (a) and unbinding (b). Solid squares: experimental data of G49R in salting-in process; Solid line: fitting curve.

TABLE I Thermodynamic constants of G49R secondary structures during salting-in process derived at the different wavenumbers.

Wavenumber/cm^{-1}	ΔH	ΔS	ΔST
1630 (β-sheet)	335±51	1155±178	344±53
1640 (Random coil)	307±49	1063±182	316±54
1650 (α-helix)	847±20	2883±66	859±19

ΔH, ΔST in kJ/mol with T=298 K, ΔS in J/(mol K).

ΔH^{in} could not be obtained because their native-states were not well defined due to lack of a clear rising phase in the thermal titration curve. There is no salting-in process in Glu for the complete exposure of molecule to the salt ions.

For the ion unbinding process, the corresponding equilibrium constant K^{u} is written as:

$$K^{\text{u}} = \frac{k_{+1}^{\text{u}}}{k_{-1}^{\text{u}}} = \frac{[\text{Unbinding state}]}{[\text{Binding state}]} \tag{8}$$

Similar to the method of treating the salting-in process, Van't Hoff plot of unbinding process for G49R is given in Fig.4(b) as an example and thermodynamic

DOI:10.1088/1674-0068/22/06/556-562

TABLE II Thermodynamic constants for ion unbinding process derived at the named wavenumbers for different samples.

	Wavenumber/cm^{-1}	ΔH	ΔS	ΔST
Glu	1617	41±8	142±26	42±7
Cyt c	1653	232±14	796±48	237±14
G49R	1640	173±10	567±32	169±9
DsbC	1640	405±22.4	1379±77	411±23

ΔH, ΔST in kJ/mol with T=298 K, ΔS in J/(mol K).

constants are listed in Table II for Glu, cyt c, G49R, and DsbC. The ΔH^{u} values of the four samples are all positive in Table II, which means that ion-unbinding is an endothermic process. The derived value of ΔH^{u} for Glu is around 41 kJ/mol, which is almost in accordance with the value of pure salt bridge unbinding [36].

In addition, ΔH^{u} values for main secondary structures are listed in Table III and IV for G49R and DsbC, respectively. The assignments of secondary structures in amide I band can be referred to Refs.[6,7,37]. Obviously, ΔH^{u} of α-helix is the largest one among ΔH^{u} values of these three secondary structures, and the interaction between ions and α-helix needs more energy to unbind. For G49R, ion-β-sheet interaction is of equal stability to ion-random coil interaction based on the fact that they have the same ΔH^{u} value within experimental error. By comparing thermodynamic constants of each kind of secondary structures for DsbC and G49R, it can be found that ΔH^{u} of DsbC is almost twice of that of G49R except for β-sheet structure, which is in agreement with that the molecular weight ratio of DsbC to G49R is 2. While ΔH^{u} values of β-sheets for DsbC and G49R are almost similar, because of the fact that there are a lot of β-sheet structures being buried in hydrophobic domain at the dimeric interface [38] and cannot interact with salt ions.

TABLE III Thermodynamic constants of G49R secondary structures for ion-protein unbinding process.

Wavenumber/cm^{-1}	ΔH	ΔS	ΔST
1630 (β-sheet)	161±31	523±99	156±29
1640 (Random coil)	173±10	567±32	169±9
1650 (α-helix)	311±48	1000±155	298±46

ΔH, ΔST in kJ/mol with T=298 K, ΔS in J/(mol K).

TABLE IV Thermodynamic constants of DsbC secondary structure for ion-protein unbinding process.

Wavenumber/cm^{-1}	ΔH	ΔS	ΔST
1630 (β-sheet)	178±24	602±80	179±24
1640 (Random coil)	405±22.4	1379±77	411±23
1650 (α-helix)	575±128	1940±432	578±129

ΔH, ΔST in kJ/mol with T=298 K, ΔS in J/(mol K).

IV. CONCLUSION

We have demonstrated for the first time that IR intensity of amide I absorption is very informative in elucidating the ion protein interaction. Generally protein in solution with salt would have a larger absorbance than that without salt. This is interpreted as ion polarizing the vibrational groups of proteins, which enhances the IR absorbance. IR absorbance thermal titration curves of proteins further reveal that there are two successive thermal activated processes of IR intensity change in salt solution when raising the temperature from 10 °C to 55 °C, corresponding to salting-in process (IR intensity increases with the raising in temperature) and ion unbinding process (IR intensity decreases with the raising in temperature). Salting-in process involves disruption of the hydrophobic interaction and the corresponding enthalpy change derived by Van't Hoff plot from the IR absorbance thermal titration reflects quantitatively the extent of hydrophobic interaction. In a similar way, the enthalpy change derived for the ion-protein unbinding process reflects the binding strength of the ions on the protein surface.

V. ACKNOWLEDGMENTS

This work was supported by the National Natural Science Foundation of China (No.20373088), the Program for Innovation Group (No.60321002), the Innovative Project of Chinese Academy of Sciences (No.KJCX2-SW-w29), and the National Key Project for Basic Research No.2006CB910302). We thank Prof. Chih-chen Wang and Dr. Hui-min Ke in the Institute of Biophysics, Chinese Academy of Science, for the preparation of samples DsbC and G49R. We also thank Prof. Xiang-gang Qiu in the Institute of physics, Chinese Academy of Sciences, for help in FTIR measurement.

[1] A. Barth and Q. C. Zscherp, Rev. Biophys. **35**, 369 (2002).
[2] S. Krimm and J. Bandekar, Adv. Protein. Chem. **38**, 181 (1986).
[3] H. Susi and D. M. Byler, Methods Enzymol. **130**, 290 (1986).
[4] W. K. Surewicz and H. H. Mantsch, Biochim. Biophys. Acta **952**, 115 (1988).
[5] J. L. Arrondo, A. Muga, J. Castresana, and F. M. Goni, Prog. Biophys. Mol. Biol. **59**, 23 (1993).
[6] M. P. Ye, Q. L. Zhang, H. Li, Y. X. Weng, W. C. Wang, and X. G. Qiu, Biophys. J. **93**, 2756 (2007).
[7] M. P. Ye, H. Li, Q. L. Zhang, Y. X. Weng, and X. G. Qiu, Chin. J. Chem. Phys. **20**, 461 (2007).

DOI:10.1088/1674-0068/22/06/556-562

[8] C. M. Phillips, Y. Mizutani, and R. M. Hochstrasser, Proc. Natl. Acad. Sci. USA **92**, 7292 (1995).
[9] R. B. Dyer, F. Gai, and W. H. Woodruff, Accounts Chem. Res. **31**, 709 (1998).
[10] R. B. Dyer, Curr. Opin. Struc. Biol. **17**, 38 (2007).
[11] L. L. Zheng, C. Guo, J. Wang, X. F. Liang, P. Bahadur, S. Chen, J. H. Ma, and H. Z. Liu, Vib. Spectrosc. **39**, 157 (2005).
[12] R. Quinn, J. B. Appleby, and G. P. Pez, J. Am. Chem. Soc. **117**, 329 (1995).
[13] R. Vogel and F. Siebert, Biochemistry **41**, 3529 (2002).
[14] R. Vogel, Curr. Opin. Colloid Interface Sci. **9**, 133 (2004).
[15] L. A. Sikkink and M. Ramirez-Alvarado, Biophys. Chem. **135**, 25 (2008).
[16] W. D. Kohn, C. M. Kay, and R. S. Hodges, J. Mol. Biol. **267**, 1039 (1997).
[17] Y. Goto, N. Takahashi, and A. L. Fink, Biochemistry **29**, 3480 (1990).
[18] R. Vogel and F. Siebert, Biochemistry **41**, 3536 (2002).
[19] K. Sakurai, M. Oobatake, and A. Y. Goto, Protein Sic. **10**, 2325 (2008).
[20] H. Ke, S. Zhang, J. Li, G. J. Howlett, and C. C. Wang, Biochemistry **45**, 15100 (2006).
[21] W. W. Wright and J. M. Vanderkooi, Biospectroscopy **3**, 457 (1997).
[22] D. M. Kim and J. R. Swartz, Biotechnol. Bioeng. **85**, 122 (2004).
[23] A. Dong, P. Huang, and W. S. Caughey, Biochemistry **29**, 3303 (1990).
[24] R. Perez-Jimenez, R. Godoy-Ruiz, B. Ibarra-Molero, and J. M. Sanchez-Ruiz, Biophys. J. **86**, 2414 (2004).
[25] D. J. Lockhart and P. S. Kim, Science **260**, 198 (1993).
[26] L. Onsager, J. Am. Chem. Soc. **58**, 1486 (1936).
[27] L. Onsager, J. Phys. Chem. **43**, 189 (1939).
[28] W. H. Furry, R. C. Jones, and L. Onsager, Phys. Rev. **55**, 1083 (1939).
[29] A. D. Buckingham, T. Schaefer, and W. G. Schneider, J. Chem. Phys. **32**, 1227 (1960).
[30] A. D. Buckingham, Trans. Faraday Soc. **56**, 753 (1960).
[31] A. D. Buckingham, Proc. R. Soc. Lon. Ser-A **255**, 32 (1960).
[32] R. Zangi, M. Hagen, and B. J. Berne, J. Am. Chem. Soc. **129**, 4678 (2007).
[33] F. A. Long and W. F. Mcdevit, Chem. Rev. **51**, 119 (1952).
[34] A. K. Dioumaev and M. S. Braiman, J. Am. Chem. Soc. **117**, 10572 (1995).
[35] Y. Umebayashi, T. Fujimori, T. Sukizaki, M. Asada, K. Fujii, R. Kanzaki, and S. Ishiguro, J. Phys. Chem. A **109**, 8976 (2005).
[36] H. R. Bosshard, D. N. Marti, and I. Jelesarov, J. Mol. Recog. **17**, 1 (2004).
[37] H. Li, H. M. Ke, G. P Ren, X. G. Qiu, Y. X. Weng, and C. C. Wang, Biophys. J. **93**, 2756 (2009).
[38] A. A. McCarthy, P. W. Haebel, A. Torronen, V. Rybin, E. N. Baker, and P. Metcalf, Nat. Struct. Biol. **7**, 196 (2000).

DOI:10.1088/1674-0068/22/06/556-562